Microwave absorption in insulating dielectric ionic crystals including the role of point defects

Binshen Meng and Benjamin D. B. Klein
Department of Electrical and Computer Engineering, University of Wisconsin, Madison, Wisconsin 53706

John H. Booske
Department of Electrical and Computer Engineering and Materials Science Program, University of Wisconsin, Madison, Wisconsin 53706

Reid F. Cooper
Department of Materials Science and Engineering and Materials Science Program, University of Wisconsin, Madison, Wisconsin 53706

(Received 13 October 1995)

A theoretical model of microwave absorption in linear dielectric (nonferroelectric) ionic crystals that takes into account the presence of point defects has been synthesized and specifically applied to NaCl single crystals by considering all relevant interaction mechanisms between a harmonic electric field and single-crystal ionic crystalline solids, including ionic conduction, dielectric relaxation, and multiphonon processes. The loss factor ϵ'' has been measured by a cavity resonator insertion technique for nearly pure and Ca^{2+} doped NaCl single crystals at frequencies from 2 to 16 GHz and at the temperatures from 300 to 700 K. The experimental results are in good agreement with the theoretical model. The theoretical model predicts a transition between low- and high-temperature absorption processes that may partly account for the phenomenon of thermal runaway observed during microwave processing of ceramics.

I. INTRODUCTION

Electromagnetic radiation dissipation in insulating single ionic crystals has been extensively studied in both low-[1–5] ($\leqslant$1 MHz) and high-[6–8] ($\geqslant$100 GHz) frequency regimes where the problem is simplified by dominant coupling to a single absorption mechanism or class of mechanisms. For example, at low frequencies, ionic conduction and dielectric relaxation mechanisms have been experimentally isolated, studied and characterized, including the effects of impurities.[1–4,9] At frequencies above 30 GHz and in relatively pure single crystals, electromagnetic radiation absorption is dominated by multiphoton absorption mechanisms.[6–8] However, to our knowledge, there still does not exist a quantitative, experimentally verified theory describing electromagnetic absorption in the microwave band, which must include the dependence on frequency, temperature, and type and density of point defects. An understanding of the absorption of microwave radiation by ionic crystalline solids is crucial to several materials applications of growing interest and importance, namely (1) materials selection and fabrication for advanced radomes as well as window and insulator structures in high-power coherent microwave sources, (2) microwave processing of ceramics, and (3) determining the complex dielectric properties of ceramic substrate materials for use in microwave and high-speed digital circuits. Our primary motivation for the work described in this paper was to create a theory of microwave absorption that would make quantitative predictions with a reasonably high degree of accuracy, which would be immediately useful in the above applications.

One specific example of a materials application of this work concerns the phenomenon of thermal runaway (local or global) encountered during microwave heating of ceramics[10] for purposes of sintering, bonding, or compound synthesis. The problem is most prevalent in ceramics such as alumina, where empirical measurements of the imaginary part of the dielectric constant as a function of temperature [$\epsilon''(T)$] consistently indicate a threshold temperature T_t, below which $\epsilon''(T)$ increases at a relatively modest rate, and above which it increases very rapidly. At ceramic sintering temperatures the dominant heat loss mechanism is radiation, but above T_t the microwave energy absorption increases with T much more rapidly than the system can radiatively dissipate the energy. At this point, the heated object tends to thermally ''run away'' until melting occurs.

Although an abruptly nonlinear temperature dependence of $\epsilon''(T)$ has been empirically observed in numerous ceramic materials, there has been no theoretical explanation, to date, of this type of behavior. Another motivation for this work, then, was to provide a theory that could explain thermal runaway.

In this paper, we describe a composite theoretical model for microwave radiation absorption in insulating ionic crystalline solids. This model combines the effects of several absorption mechanisms by extrapolating them to the microwave frequency range and summing each of their contributions. We then present illustrative experimental verifications of this model using NaCl single crystals with varied concentrations of cation impurities (Ca^{2+}) over the temperature range 300–700 K and the frequency range 2–16 GHz.

II. THEORETICAL MODEL

Electromagnetic energy absorption in ionic crystalline dielectric solids (i.e., in materials with no significant magnetic-

field response) can generally be associated with Ohmic loss, dielectric loss, and photon-phonon interactions. The first is due to electrical conduction of mobile charges, the second is due to the relaxation of polarized bound charges, and the third is due to the coupling between electromagnetic waves and the vibrational modes of the ionic lattice. In general, the time-averaged power dissipated per unit volume in a material can be expressed as $P_{\text{loss}}=\frac{1}{2}\omega\epsilon_0\epsilon''E^2$, where ϵ'' is the imaginary part of the (relative) complex dielectric constant of the material, ω is the angular frequency of the electric field E, and ϵ_0 is the permittivity of free space. The complex and frequency-dependent dielectric constant $\epsilon=\epsilon_0(\epsilon'-i\epsilon'')$ is determined by the structural properties and thermodynamic state of the material.

At frequencies and temperatures of interest for many of the applications cited above (i.e., frequencies between 1 and 30 GHz and temperatures between 300 K and approximately half the melting temperature) there is no known single dominant electromagnetic dissipation mechanism in ionic crystalline solids. On the basis of existing theories, the total absorption will always be expected to take the form of a sum of contributions from all of the major absorption mechanisms in ionic crystals, although when one mechanism is dominant the others may be ignored. In our case, none of the mechanisms can be safely ignored, and ϵ'' must be written in the more general form

$$\epsilon''=\epsilon_c''+\epsilon_d''+\epsilon_{\text{mp}}'', \tag{2.1}$$

where ϵ_c'', ϵ_d'' and ϵ_{mp}'' represent contributions from ionic conduction, dielectric relaxation, and multiphonon processes, respectively. Theoretical model expressions for each of these mechanisms have been developed and experimentally verified in studies in significantly different frequency regimes where the coupling to a single mechanism is dominant, and the other mechanisms can either be ignored or subtracted out.[1–8] To create a model expression for absorption at centimeter wavelengths, these individual expressions have been extrapolated into the frequency range of interest and added. The development of the expressions and our use of them is discussed in further detail below. All derivations are done for the example of NaCl, which is the material used in our experimental work; however, it is clear that this theory could easily be applied to other ionic crystalline materials as well.

A. Ionic conduction

The imaginary part of the dielectric constant contributed by electrical conduction is conventionally given by[11]

$$\epsilon_c''=\frac{\sigma}{\omega\epsilon_0}, \tag{2.2}$$

where σ is the electrical conductivity and ω is the microwave frequency. In NaCl crystals, the most important mechanism of electrical conduction results from ion migration in the presence of an external electrical field. This is made possible by the existence of both intrinsic and extrinsic point defects that allow both cations and anions to be able to jump among their equivalent lattice sites. However, given that NaCl is a Schottky-disorder compound, i.e., one where cation and anion vacancies dominate the intrinsic point defect equilibrium, and since the ions contributing to the conductivity are therefore those with neighboring vacancies, we can equivalently treat the vacancies as the charge carriers. Calculations based on this model lead to a thermally activated expression for ionic conductivity,[11] which includes contributions from both anion and cation vacancy migration. In our model, we choose to neglect the contribution to the ionic current due to the motion of anion vacancies. The reason for this is that for our illustration with NaCl, the enthalpy of anion vacancy migration is on the order of 0.1 eV greater than that of cation vacancy migration.[4,5] This means that the part of ϵ_c'' contributed by the anion vacancy migration will be smaller than the cation vacancy contribution by a factor of $e^{-0.1/kT}$, which is one (at 400°C) to two (at 20 °C) orders of magnitude smaller over our experimental temperature range. Also, the anion vacancy concentration is depressed relative to the cation vacancy concentration by the presence of divalent cation substitutional impurity ions (which have been experimentally detected in non-negligible concentrations even in the nominally pure samples). Our final expression for ϵ_c'' is[11]

$$\begin{aligned}\epsilon_c''&=\frac{n_c e^2 b^2 \nu_0}{\omega\epsilon_0 kT}e^{-\Delta g_{m,c}/kT}+\frac{n_a e^2 b^2 \nu_0}{\omega\epsilon_0 kT}e^{-\Delta g_{m,a}/kT}\\&\approx\frac{n_c e^2 b^2 \nu_0}{\omega\epsilon_0 kT}e^{-\Delta g_{m,c}/kT},\end{aligned} \tag{2.3}$$

where n_c is the free cation vacancy number density, n_a is the free anion vacancy number density, b is the vacancy jump distance ($b=3.99$ Å), ν_0 is some characteristic lattice frequency,[4] $\Delta g_{m,c}(=\Delta h_{m,c}-T\Delta s_{m,c})$ is the Gibb's free energy for cation vacancy jumps (where $\Delta h_{m,c}$ and $\Delta s_{m,c}$ are the enthalpy and entropy for migration of a cation vacancy), and $\Delta g_{m,a}$ is the Gibb's free energy for anion vacancy jumps. In this paper we will use Δg_m, Δh_m, and Δs_m to mean $\Delta g_{m,c}$, $\Delta h_{m,c}$, and $\Delta s_{m,c}$, respectively. Both ν_0 and Δs_m contribute to the preexponential factor in Eq. (2.3) and other equations of this form; we will always use $\nu_0=4.91\times10^{12}$ (the retrahlen frequency of NaCl) and choose Δs_m accordingly. The values for all enthalpies and entropies used are presented below with some discussion.

To obtain the equilibrium number density n_c of the free cation vacancies, we must simultaneously solve the mass-action-law equations for the concentration of Schottky vacancies, vacancy-vacancy pairs, and vacancy-impurity pairs, along with enforcing overall charge neutrality.[4,11] Using standard notation (see, e.g., Kingery, Bowen, and Uhlmann[11]) and defining $x_{\text{cv}}=[V'_{\text{Na}}]$, $x_{\text{av}}=[V^{\cdot}_{\text{Cl}}]$, $x_{\text{vv}}=[V'_{\text{Na}}V^{\cdot}_{\text{Cl}}]$, $x_i=[\text{Ca}^{\cdot}_{\text{Na}}]$, $x_{\text{vi}}=[\text{Ca}^{\cdot}_{\text{Na}}V'_{\text{Na}}]$, and $\eta=[\text{Ca}^{\cdot}_{\text{Na}}]+[\text{Ca}^{\cdot}_{\text{Na}}V'_{\text{Na}}]$ (the total Ca^{2+} concentration), these equations are

$$x_{\text{cv}}x_{\text{av}}=K_f,\quad K_f=e^{-\Delta g_f/kT}, \tag{2.4}$$

$$x_{\text{vv}}=K_f K_{\text{vv}},\quad K_{\text{vv}}=Z_{\text{vv}}e^{-\Delta g_{\text{vv}}/kT}, \tag{2.5}$$

$$x_{\text{vi}}=x_i x_{\text{cv}}K_{\text{vi}},\quad K_{\text{vi}}=Z_{\text{vi}}e^{-\Delta g_{\text{vi}}/kT}, \tag{2.6}$$

$$x_i+x_{\text{av}}=x_{\text{cv}}, \tag{2.7}$$

and

$$x_i + x_{\rm vi} = \eta. \tag{2.8}$$

where $\Delta g_f = \Delta h_f - T\Delta s_f$, $\Delta g_{\rm vv} = \Delta h_{\rm vv} - T\Delta s_{\rm vv}$, and $\Delta g_{\rm vi} = \Delta h_{\rm vi} - T\Delta s_{\rm vi}$. Δh_f denotes the enthalpy of Schottky defect formation, Δs_f the entropy of Schottky defect formation, $\Delta h_{\rm vv}$ the enthalpy of cation vacancy-vacancy association, $\Delta s_{\rm vv}$ the entropy of cation vacancy-vacancy association, $\Delta h_{\rm vi}$ the enthalpy of cation vacancy-impurity association, and $\Delta s_{\rm vi}$ the entropy of cation vacancy-impurity association. $Z_{\rm vv}$ and $Z_{\rm vi}$ are the distinct numbers of orientations of the v-v and the v-i pairs, respectively, which contribute to the configurational entropy ($Z_{\rm vv}=6$ and $Z_{\rm vi}=12$ for NaCl). Note that we have assumed a single type of impurity, Ca^{2+}, in these equations (which is the impurity we doped the experimental samples with); in addition, that ideal solution theory is assumed to apply to the defect reactions due to their low concentrations (i.e., activity coefficients have been dropped).[11,12]

Among the defined concentrations, $x_{\rm cv}$ is the concentration of free cation vacancies that contribute to the conductivity. It consists of two parts. One is the concentration of intrinsic free cation vacancies, equal to $x_{\rm av}$, and the other is the concentration of extrinsic free cation vacancies, equal to x_i. Therefore, we need to solve Eqs. (2.4)–(2.8) for x_i and $x_{\rm av}$. Rearranging the equations, we have

$$K_{\rm vi}K_f x_i^3 + (k_f - \eta K_{\rm vi}K_f - K_{\rm vi}^2 K_f^2)x_i^2 - 2\eta K_f x_i + \eta^2 K_f = 0 \tag{2.9}$$

and

$$x_{\rm av} = \frac{x_i}{\eta - x_i} K_{\rm vi}K_f. \tag{2.10}$$

There exist three solutions of Eq. (2.9) mathematically. The physical solution can be expressed as

$$x_i = 2r^{1/3}\cos\left(\theta + \frac{4\pi}{3}\right) - s, \tag{2.11}$$

where

$$r = \left[-\left(\frac{p}{3}\right)^3\right]^{1/2}, \quad \theta = \tfrac{1}{3}\cos^{-1}\left(-\frac{q}{2r}\right) \tag{2.12}$$

and

$$s = \frac{1}{3}\left(\frac{1}{K_{\rm vi}} - \eta - K_a K_f\right), \tag{2.13}$$

$$p = -\frac{2\eta}{K_{\rm vi}} - \frac{1}{3}\left(\frac{1}{K_{\rm vi}} - \eta - K_{\rm vi}K_f\right)^2, \tag{2.14}$$

$$q = \frac{2}{27}\left(\frac{1}{K_{\rm vi}} - \eta - K_{\rm vi}K_f\right)^3 + \frac{2\eta}{3K_{\rm vi}}\left(\frac{1}{K_{\rm vi}} - \eta - K_{\rm vi}K_f\right) + \frac{\eta^2}{K_{\rm vi}}. \tag{2.15}$$

Finally, we solve for the number destiny of free cation vacancies that contribute to the ionic conductivity as

$$n_c = N x_{\rm cv} = N(x_i + x_{\rm av}), \tag{2.16}$$

where N is the number density of normal cation sites, x_i is obtained from Eqs. (2.11)–(2.15), and $x_{\rm av}$ is obtained from Eq. (2.10). It is evident that the vacancy density n_c is a function of temperature and other parameters, such as the formation energy for Schottky defects, the association energy for defect pairs, and the concentrations of divalent impurities in the crystal.

B. Dielectric relaxation

As mentioned previously, at a given temperature a certain fraction of vacancies and divalent impurities will be associated in defect pairs (both vacancy-vacancy pairs and vacancy-impurity pairs) because of attractive Coulomb forces. Each pair consists of two charge carriers of equal magnitude and opposite sign, so that the pair can be treated as a dipole. When an external electric field is applied, the dipoles will all eventually align themselves in the direction of the electric field. If the field is alternating, the dipoles will be reoriented at the same frequency as the applied field but will lag behind out of phase. During this process, a certain amount of electromagnetic energy is irreversibly transferred to the dipole system. This is referred to as dielectric relaxation. Since the macroscopic polarization due to dipole alignment decays exponentially in time after the application of an electric field impulse, the macroscopic dielectric constant due to dipole relaxation will take the Debye form, characterized by a relaxation time τ:

$$\epsilon'(\omega) = \epsilon_\infty + \frac{\epsilon_s - \epsilon_\infty}{1 + \omega^2\tau^2}, \tag{2.17}$$

$$\epsilon''(\omega) = \frac{(\epsilon_s - \epsilon_\infty)\omega\tau}{1 + \omega^2\tau^2}, \tag{2.18}$$

where ϵ_∞ is ϵ' at frequencies much greater than the inverse of the relaxation time, and ϵ_s is ϵ' at frequencies much less than the inverse of the relaxation time.

More generally, if the system is characterized by more than one relaxation time τ, these expressions are rewritten as the sum of several Debye terms. Breckenridge, in his pioneering work in this area, derived expressions for the dielectric constant that included both vacancy-vacancy (v-v) and nearest-neighbor (nn) vacancy-impurity (v-i) dipole pair relaxations, resulting in two relaxation times in his theory.[1,2,13] Since that time, there has been considerable attention focused on the significant concentrations of next-nearest-neighbor (nnn) vacancy-impurity pairs in NaCl (Refs. 14–17) as the binding energy of the *nnn* pair is comparable to that of the nn pair for many impurity defects, including Ca^{2+}.[16,17] This extended theory results in three relaxation times, one for v-v pairs and two for v-i pairs.[15] However, according to the work of Dreyfus and Laibowitz,[16] one of the v-i relaxations can be expected to have a peak absorption magnitude about 25 times smaller than that of the other v-i relaxation for NaCl doped with Ca^{2+}. Many experimental results confirm that this system is well characterized by a single relaxation time.[13–20] Similarly, the v-v relaxation absorbs far less than the dominant v-i relaxation in the doped case. We do not ignore the contribution of v-v pairs in our theory, however, because as can be seen from Eq. (2.5) the concentration of v-v pairs is independent of the dopant concentration (to first order), so this relaxation will have a more

important contribution in almost pure crystals. We therefore initially chose to use Breckenridge's two relaxation time model. If one wanted to include the third relaxation term, it would not present any serious difficulty; Eqs. (2.4)–(2.8) would retain the same form if K_{vv} were replaced by $K_{eff}=K_{vv}^{(nn)}+K_{vv}^{(nnn)}$, and the individual concentrations of each type of v-i pair could be determined if the relative rate of nn to nnn and nnn to nn jumps was known.[14]

If we assume that in both v-i and v-v pair relaxations only the jumps of one nn vacancy to other nn lattice sites (w_1-type jumps[14]) are important, we can follow Breckenridge[1,2] and Lidiard[13,14] to derive the following expression for the macroscopic polarization of the material containing v-v and v-i pairs due to an applied time-harmonic electric field ($E=E_0e^{j\omega t}$):

$$P=\frac{Ne^2a^2E}{6kT}\left(\frac{x_{vv}}{2(1+j\omega\tau_{vv})}+\frac{x_{vi}}{1+j\omega\tau_{vi}}\right) \tag{2.19}$$

where N, x_{vv}, and x_{vi} are defined in Sec. II A, a is the lattice constant for NaCl, τ_{vv} is the relaxation time for v-v pairs, and τ_{vi} is the relaxation time for v-i pairs. The relaxation times are functions of temperature as follows:

$$\tau_{vv}=\frac{1}{4\nu_0}e^{\Delta g_{mvv}/kT} \tag{2.20}$$

and

$$\tau_{vi}=\frac{1}{2\nu_0}e^{\Delta g_{mvi}/kT}, \tag{2.21}$$

where Δg_{mvv} and Δg_{mvi} are the Gibbs free energies for the w_1-type vacancy jumps around another vacancy and an impurity, respectively. In order to obtain the imaginary part of the dielectric constant, we make use of Eq. (2.19) and the Clausius-Massotti relation between the microscopic polarizability and the macroscopic dielectric constant[1,9] to obtain

$$\epsilon_d''=\frac{Nx_{vv}e^2a^2(\epsilon_\infty+2)^2}{54\epsilon_0kT}\frac{\omega\tau_{vv}}{1+\omega^2\tau_{vv}^2}+\frac{Nx_{vi}e^2a^2(\epsilon_\infty+2)^2}{28\epsilon_0kT}\frac{\omega\tau_{vi}}{1+\omega^2\tau_{vi}^2}. \tag{2.22}$$

For NaCl, $\epsilon_\infty=6$.[1] Note that this expression has the required form of a sum of two Debye curves.

Similar to the contribution from ionic conduction discussed earlier, the contribution from the ion jump relaxation process is very temperature sensitive. However, the magnitude of ϵ_d'' is typically greater than ϵ_c'' by several orders of magnitude, except at high temperatures in relatively pure crystals.

C. Multiphonon quasiresonant process

In addition to the above mechanisms, photon-phonon interactions are another important class of mechanisms that contribute to electromagnetic energy absorption in ionic crystals. They are the dominant absorption mechanism in the high-frequency range (millimeter wave and far infrared). However, their contribution in the frequency range of 2–20 GHz cannot be ignored, particularly in relatively pure crystals with low point defect concentrations. For the specific case of crystalline materials with the rocksalt structure, multiphonon absorption of microwave energy is dominated by a lifetime-broadened two-phonon difference process.[6,7] Based on the work in Refs. 6 and 7 ϵ_{mp}'' can be calculated as

$$\epsilon_{mp}''=\frac{(\epsilon_s-\epsilon_\infty)\omega_f^3\Gamma}{(\omega^2-\omega_f^2)^2+(\omega_f\Gamma)^2}, \tag{2.23}$$

where ω_f is the resonant frequency of the fundamental reststrahlen transverse-phonon mode. Note that while ϵ_s and ϵ_∞ are still interpreted as the low- and high-frequency dielectric constants, respectively, they will have different numerical values in this calculation than in the dielectric relaxation calculation. This is due to the fact that the two-phonon absorption peaks at a much higher frequency than the dielectric relaxation absorption. The relaxation rate constant Γ corresponding to the reststrahlen mode is given by

$$\Gamma=\int_0^{k_{BZ}}dkg(k)L(\mathscr{E}). \tag{2.24}$$

where $g(k)$ is determined by the geometry and structure of the crystal, and $L(\mathscr{E})=\gamma/\pi\hbar/[(\omega_{ji}-\omega)^2+\gamma^2]$ is a normalized Lorentzian function with $\mathscr{E}=\hbar\omega-\hbar\omega_{ji}$, and $\omega_{ji}=\omega_j-\omega_i$.[6]

However, Eq. (2.24) is not very useful for the actual calculation of the temperature dependence of Γ. In Ref. 6, a more useful approximate expression is derived from the above, which is

$$\Gamma=\frac{2}{\pi}\Gamma_0\left[\arctan\left(\frac{\omega_f-\omega}{\gamma}\right)-\arctan\left(\frac{\omega_c-\omega}{\gamma}\right)\right], \tag{2.25}$$

where

$$\Gamma_0=\Gamma_\infty\tilde{n}\left(\frac{k_0}{k_{BZ}}\right)^2\left(\frac{\omega_m^3}{\omega_i\omega_j(\omega_f-\omega_c)}\right)\sin^2\left(\frac{\pi k_0}{2k_{BZ}}\right) \tag{2.26}$$

and

$$\Gamma_\infty=\pi N_Bh\phi_3^2/6M_rM_<M_>\omega_f\omega_m^3, \tag{2.27}$$

$$\tilde{n}=\overline{n(\omega_i)}-\overline{n(\omega_i+\omega)}, \tag{2.28}$$

and

$$\overline{n(\omega_i)}=\left[\exp\left(\frac{\hbar\omega_i}{k_BT}\right)-1\right]^{-1}\approx\frac{k_BT}{\hbar\omega_i}-\frac{1}{2}, \tag{2.29}$$

where ω is the frequency of the microwave radiation, and T is the temperature. The constants are to be interpreted as follows:[6] k_0 is the ''energy-conserving'' wave number, k_{BZ} is the wave number at the Brillouin-zone boundary in the [111] direction ($k_{BZ}=9.65\times10^7$ rad/cm), ω_i is the frequency of the acoustic phonon contributing to the relaxation, ω_j is the frequency of the optical phonon contributing to the relaxation, γ is the sum of the relaxation frequencies of the acoustic and optical phonons i and j, ω_c is the frequency difference between the transverse optic and the transverse acoustic phonon dispersion curve branches at the Brillouin-zone boundary, ω_m is the maximum frequency of the

TABLE I. Values of material parameters of NaCl relevant to two-phonon lifetime-broadened absorption (Ref. 6).

Material parameter (dimensions)	Value	Material parameter (dimensions)	Value
ϵ_s (dimensionless)	5.9	N_B(dimensionless)	20
ϵ_∞ (dimensionless)	2.33	$\phi_3(10^{12}$ erg/cm$^3)$	−5.93
γ (cm^{-1})	18	M_r (10^{-23} g)	2.32
ω_f (cm^{-1})	164	$M_<$ (10^{-23} g)	3.82
ω_c (cm^{-1})	20	$M_>$ (10^{-23} g)	5.89
ω_m (cm^{-1})	115		

acoustic phonon branches at the Brillouin-zone boundary, N_B is the total number of phonon branches that contribute to the relaxation, ϕ_3 is the third derivative of the lattice potential evaluated at a lattice site, $M_<$ is the mass of the less massive lattice ion, $M_>$ is the mass of the more massive lattice ion, and M_r is the reduced mass of the pair, which is simply the product of the ion masses divided by the sum of the ion masses. Over the frequency range examined in this research, $\omega \ll \omega_c$, and therefore we can take $k_0 = k_{\mathrm{BZ}}$, $\omega_i = \omega_m$, and $\omega_j = \omega_m + \omega$.[6] The values of the constants used are listed in Table I. All of the values quoted in Table I are from Ref. 6, except N_B, which was not explicitly stated in the article. We obtained the listed value by fitting the calculated $\Gamma(T)$ curve to the data points presented in that article. Reference 6 contains a discussion of the determination of their value of γ, which we used in our calculations.

Calculations with the above expressions predict absorption as a function of temperature in good agreement with experimental results in the millimeter-wave frequency range, $f > 30$ GHz.[6] Extrapolations down into the lower microwave region, 2–20 GHz, show that ϵ''_{mp} varies much less sensitively with temperature than contributions from ionic conductivity or ion jump relaxation in this frequency range. In particular, ϵ''_{mp} varies approximately linearly with both temperature and frequency.

III. EXPERIMENTAL RESULTS AND COMPARISON TO THEORY

A. Experimental method

To evaluate our theoretical model of microwave absorption experimentally, we have measured ϵ'' in NaCl as a function of temperature, frequency, and Ca^{2+} impurity dopant concentration. The measurements were performed on cylindrical single-crystal specimens by measuring the change in the loaded Q of a temperature-controlled cylindrical cavity resonator due to a sample inserted in a small hole in the top of the cavity. The experimental configuration is described in detail in Ref. 21. A 2–26 GHz synthesized signal generator was used as a precise microwave excitation source. Two resonant cavities and several modes in each were employed to provide measurements at five frequencies spanning the range of 2–20 GHz. To ensure that the NaCl specimen was isothermal, the entire cavity was resistively heated, surrounded by thermal insulation, and placed inside an evacuated chamber to prevent oxidation. At the higher frequencies and higher-order radial eigenmodes, the sample diameter was not sufficiently small to use conventional cavity perturbation analysis without incurring unacceptably large errors. Hence an extended form of the cavity perturbation theory[22] was employed for data analysis to obtain higher accuracy in the measurements of ϵ''.

Four high-purity circular cylindrical rod-shaped NaCl single-crystal specimens were commercially obtained (Harshaw) and prepared for the measurements: (1) 4-mm diameter, as received; (2) 4-mm diameter, doped with Ca^{2+} to an estimated level of 200–400 ppm; (3) 3-mm diameter, as received; and (4) 3-mm diameter, doped with Ca^{2+} to an estimated level of 50–200 ppm. Samples (1) and (2) were used for the larger cavity with lower resonant frequencies (approximately 2, 5, and 8 GHz), and samples (3) and (4) were used with the smaller cavity with higher resonant frequencies (approximately 5, 11, and 18 GHz). The redundancy near 5 GHz was intentional to cross check that both cavities yielded identical data at this frequency (for the undoped reference samples). After inserting the samples into the cavities, the resonant frequencies were shifted from the empty cavity values down to 2.2, 4.8, and 7.4 GHz for the low-frequency cavity and 4.8, 10.2, and 15.5 GHz for the high-frequency cavity. From these frequency shifts the value of ϵ' can be determined;[22] we calculated it be 5.63 ± 0.05 in every case. Measurements of ϵ'' were performed over the temperature range of 300–700 K by taking data in 40 K increments. The relative measurement error was established[21] to be $\pm 1\%$.

B. Impurity concentrations

In order to compare the theoretical results to the experimental measurements, we must have the values of several parameters required by Eqs. (2.3)–(2.22). The first of these parameters is the impurity concentration. By using inductively coupled plasma (ICP) spectroscopy (Wisconsin State Laboratory of Hygiene), the impurity concentrations of all samples were measured. The concentrations of many of the impurities that were investigated were negligible, falling close to or below the detection limits. In particular, seven elements (As, Be, Cr, Co, Ni, Tl, and V) were indicated as below the detection limit. The presence of ten more elements was possibly suggested, but (within the error limits) at concentrations too small to be significant for our purposes (e.g., Al 209.3 ± 104.6 (ppm), Sb 7.81 ± 47.55, Ba 0.4005 ± 0.9250, Cd 0.3559 ± 0.6370, Cu 8.328 ± 7.995, Fe 10.47 ± 6.502, Pb 12.76 ± 28.06, Mn 1.704 ± 0.784, Mo 4.894 ± 9.298, and Se 41.30 ± 80.95, in the undoped samples). Four elements were detected in concentrations that could be significant to our results: Ca (the dopant impurity), Mg, K, and Zn. Their concentrations are listed in Table II. It is com-

TABLE II. Impurity concentrations in the NaCl samples determined by an inductively coupled plasma technique (in Wisconsin State Laboratory of Hygiene). *L* represents concentrations below the detection limit of the measurement system. ppm here refers to the mole fraction.

Impurity element	Concentration (ppm) in samples 1 & 3	Concentration (ppm) in doped sample 4	Concentration (ppm) in doped sample 2
Ca	19.76 ± 17.32	151.7 ± 20.1	375.2 ± 30.1
Mg	160.9 ± 363.6	*L*	*L*
K	1736 ± 1858	1523 ± 3823	801.8 ± 2533.7
Zn	37.17 ± 1.32	37.39 ± 5.21	27.38 ± 1.24

mon practice to assume that elements whose error bounds are comparable to their mean estimated concentration have negligible concentrations (clearly this must be done in the context of other information such as the crystal-growth conditions, which was provided by the manufacturer). We therefore neglected the possible presence of Mg and K in the samples. This assumption is further justified in light of our experimental and theoretical results. A possible large concentration of K in the samples will not affect our results significantly, as it will only produce a secondary effect on the ionic conductivity, and as is shown in Fig. 2, the contribution of ionic conduction to our measured microwave absorption was only important at the highest temperatures and lowest frequencies tested in our experiments. We can discount the presence of a large concentration of Mg, as such a concentration in the undoped samples (1 and 3) would have had a significant effect on the microwave absorption. The fact that we obtained a good theoretical fit to the data while assuming a fairly low divalent impurity concentration eliminates the possibility of anything like 160 ppm of Mg being present in the samples. The remaining elements with clearly non-negligible concentrations are Ca for (the doped) samples 2 and 4, and a surprising baseline presence of Zn in all three samples.

The simultaneous presence of two types of divalent impurities, in this case Ca^{2+} and Zn^{2+}, is not dealt with in our theory as developed above. In general, the two types of impurities would not be expected to have identical defect parameters ($\Delta h_{\rm vi}$, $\Delta s_{\rm vi}$, $\Delta h_{m\rm vi}$, and $\Delta s_{m\rm vi}$), and therefore Eqs. (2.4)–(2.8) must be reformulated with this in mind (a straightforward but tedious exercise). In addition, there will be an additional v-i relaxation term due to the Zn^{2+} which will contribute to the total absorption. The difficulty with this problem is that Zn^{2+} in NaCl, unlike Ca^{2+} in NaCl, is not a fully characterized system. There are only a few references which attempt to give the defect parameters.[15,23,19] On the basis of simplified Coulombic arguments one would expect that the defect parameters would be similar to those of Ca^{2+}, as both are divalent impurities. The defect parameters given for Zn^{2+} in NaCl are indeed similar to those of Ca^{2+} in NaCl.[15,19] For our purposes, we chose effectively to treat the Zn^{2+} impurities as Ca^{2+} impurities. When performing theoretical calculations, the Ca^{2+} concentration was fixed at the value of 40 ppm for samples 1 and 3, 405 ppm for sample 2, and 190 ppm for sample 4. These values were obtained from Table II by adding the concentrations of Ca^{2+} and Zn^{2+} for each sample. It should be noted that the concentration of Ca^{2+} in samples 1 and 3 was taken to be negligible, in accordance with our convention of dropping impurity concentrations which are comparable to the error bounds.

TABLE III. Enthalpies and entropies used.

Process	Enthalpy (eV)	Entropy (k)
Cation vacancy migration	$\Delta h_m = 0.70$	$\Delta s_m = 1.87$
Schottky defect formation	$\Delta h_f = 2.41$	$\Delta s_f = 8.896$
Cation v-v pair association	$\Delta h_{\rm vv} = -0.865$	$\Delta s_{\rm vv} = -1.2$
Cation v-i pair association	$\Delta h_{\rm vi} = -0.612$	$\Delta s_{\rm vi} = -2.508$
Cation v-i pair activation	$\Delta h_{m\rm vi} = 0.70$	$\Delta s_{m\rm vi} = 1.87$

C. Enthalpy and entropy values

The other parameters required for our theoretical calculations are the various enthalpies and entropies of formation and activation for point defects and point-defect pairs. As a starting point, we used the values measured by Hooton and Jacobs,[4] as these are very recent and are in good agreement with values found elsewhere. We found that the v-v relaxation term from Eq. (2.22) did not make a significant contribution to our calculated values for any reasonable values of the activation parameters ($\Delta h_{m\rm vv}$ and $\Delta s_{m\rm vv}$). It was therefore safe to ignore this term in our calculations. Following Dryden and Heydon,[20] we assumed the same values for the enthalpy and entropy of cation vacancy motion around the Ca^{2+} impurities as for the motion through the undisturbed lattice (i.e., $\Delta h_{m\rm vv} = \Delta h_m$, and $\Delta s_{m\rm vi} = \Delta s_m$).

These initial values for the enthalpies and entropies did not result in a good fit to our experimental results, however. We noted that there is considerable variation in the literature

TABLE IV. Some measured values of Δh_m, $\Delta h_{m\rm vv}$, and Δs_m by others.

Δh_m (eV)	$\Delta h_{m\rm vi}$ (eV)	Δs_m (k)	Reference
0.626		1.065	4
0.65 ± 0.01		1.7 ± 0.1	24
0.69		1.64	5
0.715		3.3	27
0.75 ± 0.01			28
0.678	0.678	1.87	20
	0.695		25
	0.70		19
	0.72		26

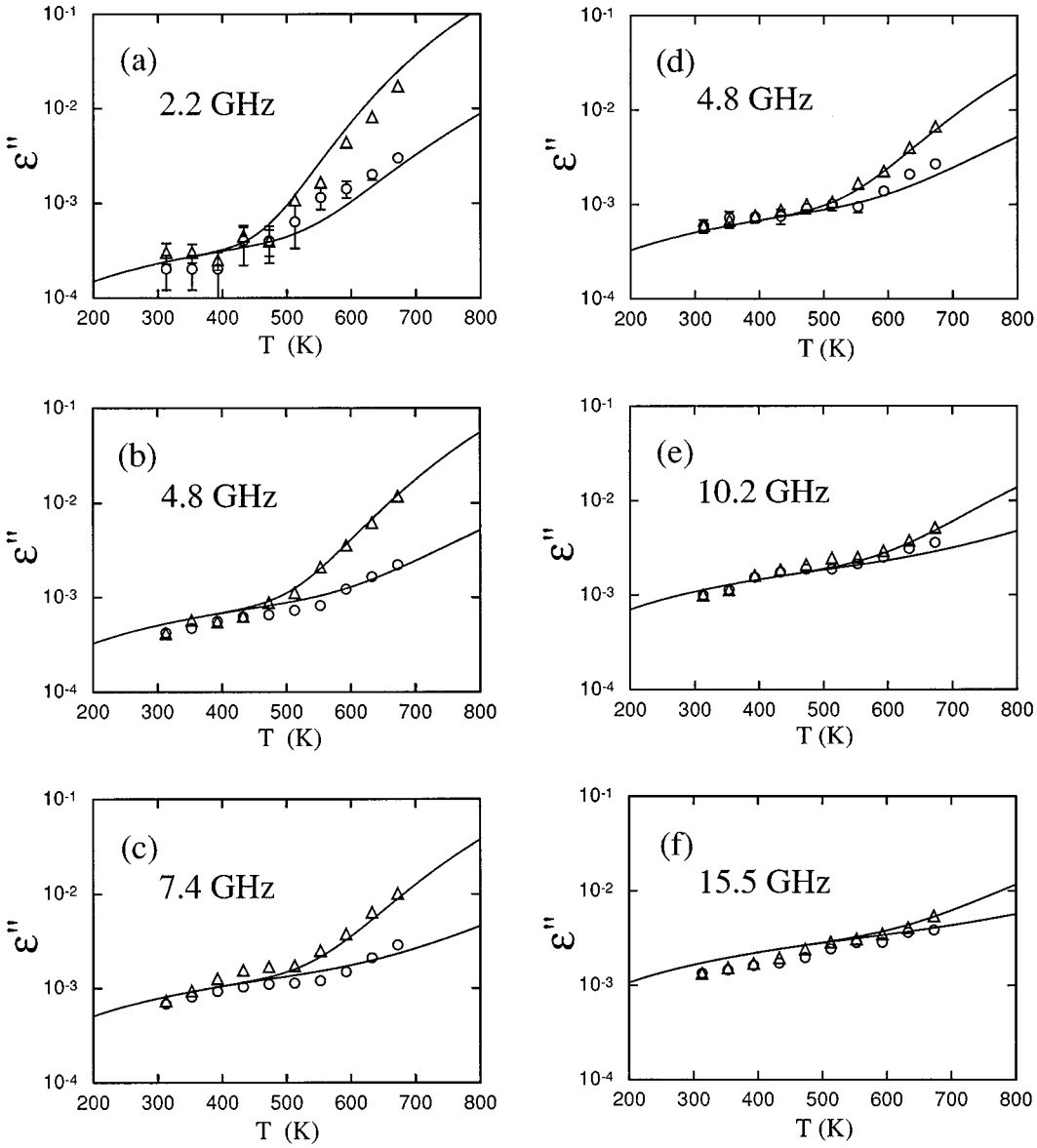

FIG. 1. The experimentally measured ϵ'' and theoretically predicted ϵ'' in NaCl single crystals at the frequencies of (a) 2.2 GHz, (b) 4.8 GHz, and (c) 7.4 GHz vs temperature for the first cavity, and (d) 4.8 GHz, (e) 10.2 GHz, and (f) 15.5 GHz vs temperature for the second cavity. In all the plots, the symbols are as follows. ○: undoped crystal (nearly pure crystals). Δ: doped crystals. —: theory with 40-ppm effective Ca^{2+} for the undoped sample and 405-ppm Ca^{2+} doping level for the doped sample, respectively, for the first cavity; theory with 40-ppm effective Ca^{2+} for the undoped sample and 190-ppm Ca^{2+} doping level for the doped sample, respectively, for the second cavity.

values of Δh_m and Δs_m, and these parameters seemed to be a natural choice to adjust in order to improve the fit. We obtained a good fit using the set of parameter values listed in Table III. For comparison, in Table IV we list some literature values for the adjusted parameters (Δh_m and Δs_m) from which we selected our values, along with values of $\Delta h_{m\mathrm{vi}}$ in order to validate our assumption that $\Delta h_{m\mathrm{vi}} = \Delta h_m$.

D. Analysis of results

In Fig. 1, the experimental and theoretical results are plotted together in order to allow direct comparison. As can be seen, the agreement between the two is very satisfactory. As mentioned above, certain activation parameters had to be adjusted to fit the experimental results, but our final set of parameters is very reasonable. The two-phonon absorption parameters of Table I were not adjusted at all; the two-phonon lifetime-broadened process dominates the absorption at low temperatures, and the good agreement between theory and experiment in our own independent investigation provides additional evidence for the correctness of the theory of this process as given in Refs. 6 and 7.

An important distinguishing feature in all of the theoretical curves is the existence of a transition temperature T_t at which there is a transition from the multiphonon process being dominant to dielectric relaxation and ionic conductivity processes being dominant. Two of the theoretical curves are broken down into components to illustrate this point in Fig. 2. Generally, T_t varies with both the dopant concentration and the microwave frequency. The experimental data and the theoretical predictions are in excellent agreement regarding the value of T_t in all cases.

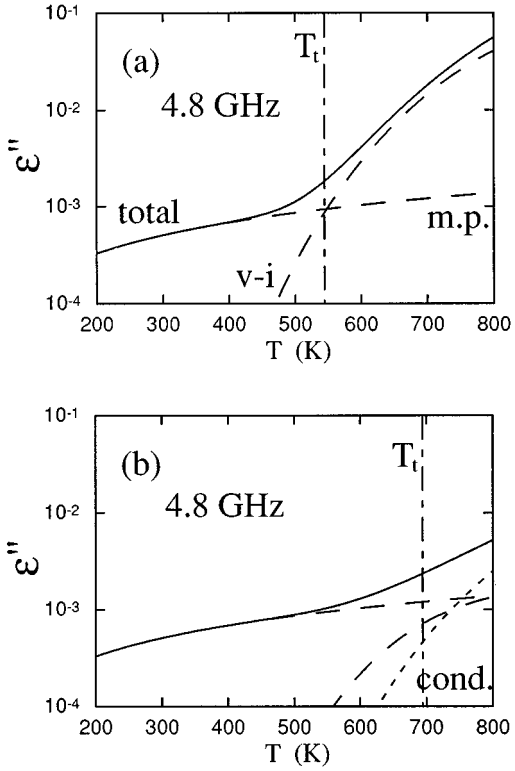

FIG. 2. The theoretical curves at 4.8 GHz from Fig. 1(b), split up into their components. The solid line is the total ϵ'', and the dashed lines are the contributions due to multiphonon processes (m.p.) and v-i pair dielectric relaxation (v-i), in both cases. (a) Doped case. (b) Undoped case, with the dotted line representing the contribution due to ionic conductivity (cond.). Also indicated on the figure is the approximate value of T_t, the transition temperature discussed in the text.

IV. SUMMARY AND CONCLUSIONS

Our theoretical starting point for this investigation was to assume that the total microwave absorption in ionic crystals could be fully explained by adding contributions from previously characterized absorption mechanisms. Based on this assumption, we generated a theoretical expression for the total microwave absorption and compared it to experimental data. The match was very good, indicating that any other possible mechanisms must make very small contributions in this frequency, temperature, and dopant range. We therefore contend that the composite model is suitable to predict the microwave absorption in any insulating linear dielectric (nonferroelectric) ionic crystal.

Based on this composite model, a possible physical explanation now exists for the abrupt onset of a highly nonlinear temperature dependence of $\epsilon''(T)$ that can lead to thermal runaway during microwave heating of ceramics. Specifically, the abrupt transition observed for ϵ'' in the microwave heating of ceramic materials[10] is observed here in NaCl. The transition temperature T_t at which this sudden increase in absorption occurs varies with defect concentrations and with frequency. In all cases, however, this phenomenon is the signature of a transition from the dominance of a weakly temperature dependent absorption mechanism—e.g., two-phonon absorption—to the dominance of thermally activated (and thus exponentially temperature dependent) absorption mechanisms, e.g., v-i pair dielectric relaxation and ionic conduction.

In addition to polar point defect pairs such as v-i and v-v pairs, in a non-single-crystal ionic solid there will also be extended defects with intrinsic polarity such as dislocations and grain boundaries. Reorientation of these extended defects would also be expected to be a thermally activated process, perhaps with much higher activation energy than that for reorientation of point defect pairs. The next stage of our research, then, is the incorporation of these processes in a theory that will predict microwave absorption in non-single-crystal ionic solids, such as polycrystalline ceramics.

ACKNOWLEDGMENTS

The authors gratefully acknowledge the partial financial support of the Electric Power Research Institute, the Wisconsin Alumni Research Foundation, and the National Science Foundation through the Presidential Young Investigator Award Program; and of Nicolet Corp. for the donation of the digital oscilloscope used in the experiments. Many valuable discussions with Sam Freeman and others are also greatly appreciated.

[1] R. G. Breckenridge, in *Imperfections in Nearly Perfect Crystals*, edited by W. Shockley, J. H. Hollomon, R. Maurer, and F. Seitz (Wiley, New York, 1952), Chap. 8.
[2] R. G. Breckenridge, J. Chem. Phys. **16**, 959 (1948).
[3] R. G. Breckenridge, J. Chem. Phys. **18**, 913 (1950).
[4] I. E. Hooton and P. W. M. Jacobs, J. Phys. Chem. Solids **51**, 1207 (1990); Can. J. Chem. **66**, 830 (1988).
[5] M. Beniere, F. Beniere, and M. Chemla, J. Phys. Chem. Solids **37**, 525 (1976).
[6] M. Sparks, D. F. King, and D. L. Mills, Phys. Rev. B **26**, 6987 (1982), and references contained therein.
[7] K. R. Subbaswamy and D. L. Mills, Phys. Rev. B **33**, 4213 (1986).
[8] V. L. Gurevich and A. K. Tagantsev, Adv. Phys. **40**, 719 (1991).
[9] I. Bunget and M. Popescu, *Physics of Solid Dielectrics* (Elsevier, Amsterdam, 1984).
[10] G. A. Kriegsmann, J. Appl. Phys. **71**, 1960 (1992), and references contained therein.
[11] W. D. Kingery, H. K. Bowen, and D. R. Uhlmann, *Introduction to Ceramics* (Wiley, New York, 1976).
[12] L. W. Barr and A. B. Lidiard, in *Physical Chemistry—An Advanced Treatise*, edited by H. Wilhelm Jost (Academic, New York, 1970), Vol. 10.
[13] A. B. Lidiard, in *Handbuch der Physik*, edited by S. Flugge (Springer-Verlag, Berlin, 1957), Vol. 20.
[14] A. B. Lidiard, *Bristol Conference Report on Defects in Crystalline Solids, 1954* (The Physical Society, London, 1955).
[15] R. W. Dreyfus, Phys. Rev. **121**, 1675 (1961).

[16] R. W. Dreyfus and R. B. Laibowitz, Phys. Rev. **135**, A1413 (1964).
[17] C. R. A. Catlow, J. Corish, J. M. Quigley, and P. W. M. Jacobs, J. Phys. Chem. Solids **41**, 231 (1980).
[18] C. H. Burton and J. S. Dryden, J. Phys. C **3**, 532 (1970).
[19] P. Varotsos and D. Miliotis, J. Phys. Chem. Solids **35**, 927 (1974).
[20] J. S. Dryden and R. G. Heydon, J. Phys. C **11**, 393 (1978).
[21] B. Meng, J. H. Booske, and R. F. Cooper, Rev. Sci. Instrum. **66**, 1068 (1995).
[22] B. Meng, J. H. Booske, and R. F. Cooper, IEEE Trans. Microwave Theory Tech. **43**, 2633 (1995).
[23] P. Suptitz and J. Teltow, Phys. Status Solidi **23**, 9 (1967).
[24] A. R. Allnatt, P. Pantelis, and S. J. Sime, J. Phys. C **4**, 1778 (1971).
[25] P. Dansas, J. Phys. Chem. Solids **32**, 2699 (1971).
[26] K. C. Kao, W. Whitham, and J. H. Calderwood, J. Phys. Chem. Solids **31**, 1019 (1970).
[27] C. Nadler and J. Rossel, Phys. Status Solidi **18**, 711 (1973).
[28] E. Laredo and E. Dartyge, J. Chem. Phys. **53**, 2214 (1970).